# Compressed Sampling based on Circulant Matrix for Analog Signals

Yanwei Xiong, Jianhua Zhang, Ping Zhang
Key Lab of Universal Wireless Communication, Ministry of Education,
Beijing University of Post and Telecommunications, Beijing, China

***Abstract*—In order to implement the high-speed data transmission in wireless communication system, the signal bandwidth becomes wider. However this results in high Nyquist sampling rate which will beyond the capacity of the hardware device. The analog-to-information conversion (AIC) based on compressed sensing (CS) is proposed to sample signals at a sub-Nyquist rate. The circulant matrix (CM) instead of the random Bernoulli matrix is used as the measurement matrix in this paper. Compared with the structure based on random Bernoulli matrix, this CM based architecture, in a certain extent, can reduce system complexity. Simulations which show the efficiency of the proposed approach are also presented.**

***Index Terms*—compressed sensing (CS), analog-to-information conversion (AIC), circulant matrix**

## I. Introduction

With the rapid development of wireless communication technology, the demand for information is increasing dramatically. The signal bandwidth becomes wider to satisfy the increasing data volume. In the traditional digital signal processing which inherently relies on sampling process, the analog-to-digital conversion (ADC)requires the sampling rate must be at least twice of the bandwidth according to the Shannon-Nyquist theorem to guarantee the reconstruction of the band-limited signal. The high frequency and high resolution ADC is one of the main performance limiters in advanced communication applications, where the bandwidth is high and the sampling rate is beyond the capacity of ADC. The acquisition hardware, the subsequent storage and digital signal processors are facing with great challenges.

Fortunately, recent work in compressed sensing (CS) provides a way to sample sparse or compressible signals efficiently at a sub-Nyquist rate [1], [2]. CS suggests that the signal characteristics can be fully captured by a number of projections which are fewer than those required by the Nyquist theorem and reconstructed perfectly from them. The sampling rate is determined based on the actual information contents rather than the signal bandwidth. This theorem has found a wide range of applications in communication, such as channel estimation, sensor network and cognitive radio.

In most practical implementations, the signal processing is divided into two steps. First, the signal is sampled at the Nyquist rate and then CS is applied to get projections. It is paradoxical because the sub-Nyquist sampling is achieved by firstly discretizing the analog signal at Nyquist rate. Actually we can avoid the discretization at Nyquist rate by applying CS to the analog signal directly. Such kind of practical method for sampling and compressing jointly is presented in [3], [4], [8], [9], [10]. [3] extends the exiting CS framework to analog signals and the analog-to-information conversion (AIC) via random demodulator has only one path. The sampling rate is lower than the Nyquist rate but is still high. Another practical sampling system which is inspired by [3] is presented in [4] and this system consists of a bank of random demodulators and ADCs running in parallel. The corresponding result is that this system has much lower sampling rate but will consume a lot of resources if the architecture contains a large number of parallel paths.

In order to provide a design flexibility and scalability, a parallel segmented structure is adopted where the analog signal is segmented [8], [9], [10]. This structure decrease the hardware resources at the expense of high sampling rate, which causes a trade off between the system complexity and sampling rate. Due to that each path is demodulated by a random demodulator which is independent with each other, that is the random Bernoulli matrix is used as the measurement matrix, it will take up much resources to generate these demodulator. In order to further reduce the resources, the circulant matrix (CM) instead of the random Bernoulli matrix (BM) is used as the measurement matrix to generate demodulators in this paper because it can be easily implemented on hardware. We also analyse the conditions that should be satisfied when the CM is used and compare the consume resources between the BM and CM. The performances of the circulant matrix based parallel segmented compressed sampling (CM-PSCS) structure for Time-Frequency signals and Multiband signals are simulated.

The remainder of this paper is organized as follows. Section II introduces the traditional discrete-time CS framework. Section III describes the analog model and the CM-PSCS structure. Simulation results are shown in section IV and conclusions are made in section V.

## II. Compressed Sensing Background

CS provides a framework for acquisition of a discrete-time signal which is sparse or compressible in some sparsity basis. It is supposed that $\mathbf{x} \in \mathbb{R}^N$ is an $N$-point real-valued discrete-time signal. Then $\mathbf{x}$ can be represented in an arbitrary basis $\{\psi_n\}_{n=1}^N$ for $\mathbb{R}^N$ with the weighting coefficients $\{\theta_n\}_{n=1}^N$. The signal $\mathbf{x}$ is represented as $\mathbf{x} = \sum_{n=1}^N \theta_n \psi_n = \mathbf{\Psi\Theta}$, where $\mathbf{\Psi}$ is an matrix using $\psi_n$ as columns, $\mathbf{\Theta}$ is the coefficient vector composed by the coefficients $\{\theta_n\}_{n=1}^N$. A signal is $K$-sparse

in the basis $\mathbf{\Psi}$ if only $K(K \ll N)$ significant elements in coefficients $\mathbf{\Theta}$ are nonzero.

The useful information in the compressed signal can be captured by the non-adaptive linear projection. The random measurement for $K$-sparse signal $\mathbf{x}$ can be expressed as $\mathbf{y} = \mathbf{\Phi x} = \mathbf{\Phi\Psi\Theta}$, where $\mathbf{y}$ is an $M \times 1$ vector and $\mathbf{\Phi}$ is an $M \times N(M \ll N)$ matrix. In order to recover the original signal $\mathbf{x}$, the matrix $\mathbf{\Phi\Psi}$ must satisfy the restricted isometry property (RIP) [1]. That is the measurement matrix $\mathbf{\Phi}$ must be incoherent with the sparse basis $\mathbf{\Psi}$. In practical applications, the elements of $\mathbf{\Phi}$ are independently drawn from a random distribution.

Recovering $\mathbf{x}$ from $\mathbf{y}$ is an ill-posed problem in general since $M \ll N$. However, due to the additional assumption that the signal $\mathbf{x}$ is sparse or compressible in the basis $\mathbf{\Psi}$, fewer measurements are sufficient to make recovery both feasible and practical. The recovery of the sparse set of significant coefficients $\mathbf{\Theta}$ can be achieved through $l_0$-norm optimization. While solving this $l_0$-norm optimization is a NP-hard problem, we can get the solution of the problem through transforming the $l_0$-norm optimization into the $l_1$-norm optimization as

$$\min ||\mathbf{\Theta}||_1 \quad s.t. \quad \mathbf{y} = \mathbf{\Phi\Psi\Theta}. \tag{1}$$

This convex optimization problem, also known as Basis Pursuit (BP) [5], can be simplified to a traditional linear programming problem. An alternative to the optimization-based approach is greedy algorithm based on dynamic programming, such as Matching Pursuit (MP) [6] and Orthogonal Matching Pursuit (OMP) [7].

## III. Compressed Sampling of Analog Signals

### A. Analog signal model

Supposing an analog signal $x(t)$ with finite information rate, it can be represented by a finite number of parameters in some continuous basis which is composed by a set of continuous functions $\{\psi_n(t)\}_{n=1}^N$ as

$$x(t) = \sum_{n=1}^{N} \theta_n \psi_n(t) = \mathbf{\Psi}(t)\mathbf{\Theta}. \tag{2}$$

with $\theta_n, t \in \mathbb{R}$, where $\mathbf{\Psi}(t) = [\psi_1(t), \cdots, \psi_N(t)]$, $\mathbf{\Theta} = [\theta_1, \cdots, \theta_N]^T$ is a vector composed of coefficients $\{\theta_n\}_{n=1}^N$. In case where there are a small number of nonzero or large magnitude entries in $\mathbf{\Theta}$, the analog signal $x(t)$ is sparse or compressible in basis $\mathbf{\Psi}(t)$ which maps the discrete vector of coefficients onto a continuous signal. Although each of the basis element $\psi_n(t)$ may have high bandwidth, the signal itself has finite information freedom. We would like to sample signals at the information rate rather than at twice the bandwidth as required by the Nyquist theorem.

### B. Analog-to-Information Converter

The AIC provides us a practical tool to acquire compressed measurements at a sub-Nyquist rate. The parallel segmented compressed sensing (PSCS) [8], [9], [10] which can provide a design flexibility and scalability on the sampling rate and system complexity consists of three main components: demodulation, integration and uniform sampling.

The analog signal $x(t)$ for $t \in [0, T]$ is segmented into $Q$ pieces $x_q(t)$, and then these pieces are fed into $P$ parallel pathes simultaneously. In the $q$th interval of the $p$th path, segment $x_q(t)$ is modulated by mixing a function $c_p(t)$ for $t \in [(q-1)T_c, qT_c]$, where $T_c = \frac{T}{Q}$. $c_p(t)$ is a $T_c$ pseudo-random number (PN) sequence of $\pm 1$'s with length of $L$. The PN sequence which can be called as chipping sequence is usually implemented using Maximal-Length Linear Feedback Shift Register (MLFSR) and its chipping rate must be faster than the Nyquist rate for the input signal $x(t)$.The MLFSR has the benefit of providing a random sequence of $\pm 1$ with zero average, while offering the possibility of regenerating the same sequence again given the initial seed. The purpose of this modulation is to provide randomness necessary for successful CS recovery.

These chipping sequences form the rows of the matrix $\mathbf{\Phi}$. Each chipping sequence $c_p(t)$ is independent and obeys the Bernouli distribution [4], [8], [9], [10], so the measurement matrix $\mathbf{\Phi}$ is a random BM whose elements are independent and identically distributed. If there are $P$ parallel paths, $P$ chipping sequences need to be constructed which results in the consumption of large amount of resources. The length of each chipping sequence is $L$, then $PL$ storage units are also needed to store them.

In order to reduce resource consumption and make it easily implemented on hardware, we utilize fully the characteristics of CM and use it as the measurement matrix. The CM-PSCS is depicted in Fig. 1.

The chipping sequence $c_p(t)$ can be obtained by 1 cyclic shift of $c_{p-1}(t)$. Supporting the chipping sequence with length of $L$ in the first path is expressed as $c_1 = [c_{1,1}, c_{1,2}, \cdots, c_{1,L}]$, the matrix $\mathbf{C}$ is composed by $c_p(t)$ as

$$\begin{aligned} \mathbf{C} &= \begin{bmatrix} c_1(t) \\ c_2(t) \\ \vdots \\ c_P(t) \end{bmatrix} \\ &= \begin{bmatrix} c_{1,1} & c_{1,2} & \cdots & c_{1,L} \\ c_{1,L} & c_{1,1} & \cdots & c_{1,L-1} \\ \vdots & \vdots & \ddots & \vdots \\ c_{1,L-Q+2} & c_{1,L-Q+3} & \cdots & c_{1,L-Q+1} \end{bmatrix}. \end{aligned} \tag{3}$$

The circulant matrix is based upon recent theoretical work on Toeplitz-structured matrix and known to satisfy the RIP [11]. The higher recovery probability will be achieved with more rows for the $P \times L$ CM. However if $P > L$, the last $P - L$ rows of the CM are the same as the first $P - L$ rows. Then no new information will be obtained by the last $P - L$ paths of the CM-PSCS.

In summary, when the CM-PSCS is adopted to sample signals, the following conditions must be satisfied:

- $\frac{L}{T_c} \geq f_s$,where $f_s$ is the Nyquist sampling frequency;
- $P \cdot Q \geq M$, where $M$ is the least number of measurements to ensure the sampled information is sufficient with

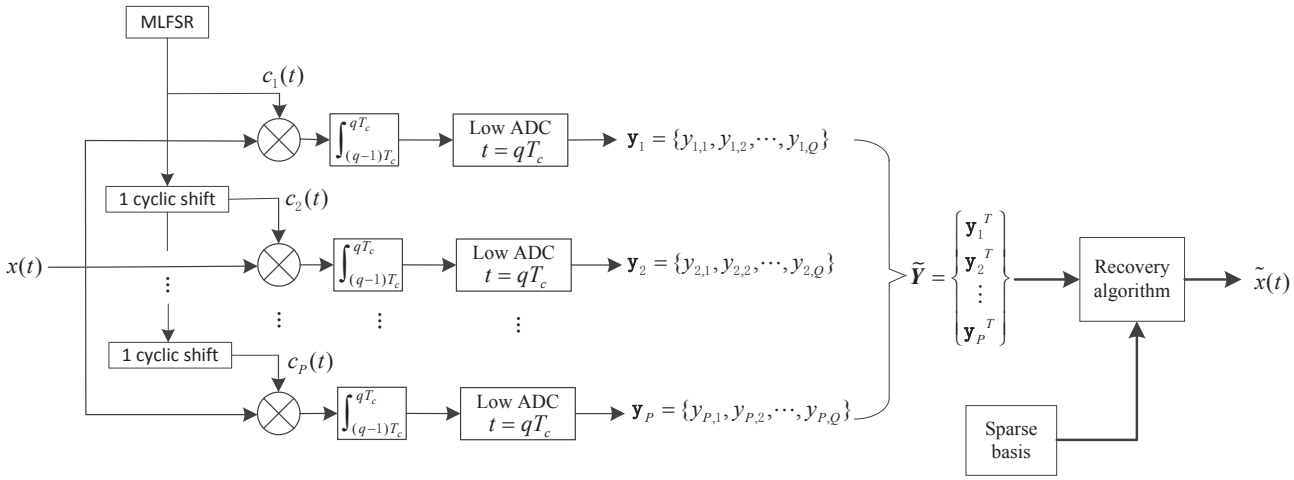


Fig. 1: The PSCS structure for AIC

TABLE I: The resources occupied by Bernoulli matrix and circulant matrix

| | Chipping sequences | Storage units |
|---|---|---|
| Bernoulli matrix | $P$ | $PL$ |
| circulant matrix | 1 | $L$ |

high probability.

- $P \leq L$, when $P = L$ the recovery probability is highest.

It can be shown from (3) that only one chipping sequence needs to be generated and the others can be obtained by simple cyclic shift of the chipping sequence.The resources occupied by BM and CM are shown in Table I. The recourses occupied by CM-PSCS structure are $\frac{1}{P}$ of those of the BM based PSCS (BM-PSCS) structure, which makes it be a better choice for the implementation on hardware.

After mixing, the piecewise integration results in the inner product of the signal $x_q(t)$ and the chipping sequence $c_p(t)$, and then the output is sampled at a low rate. The integration period of the integrator must be same as the sampling interval. After each period of $T_c$, the integrator needs to be reset.

The output $y_{p,q}$ in $q$th interval of $p$th path is given as

$$\begin{aligned} y_{p,q} &= \langle x_q(t), c_p(t) \rangle \\ &= \int_{(q-1)T_c}^{qT_c} c_p(t)x(t)dt \\ &= \sum_{n=1}^{N} \theta_n \int_{(q-1)T_c}^{qT_c} c_p(t)\psi_n(t)dt. \end{aligned} \tag{4}$$

Then the subsamples are gathered in following $P \times Q$ matrix

$$\mathbf{Y} = \begin{bmatrix} \mathbf{y}_1 \\ \mathbf{y}_2 \\ \vdots \\ \mathbf{y_P} \end{bmatrix} = \begin{bmatrix} y_{1,1} & y_{1,2} & \cdots & y_{1,Q} \\ y_{2,1} & y_{2,2} & \cdots & y_{2,Q} \\ \vdots & & & \vdots \\ y_{P,1} & y_{P,2} & \cdots & y_{P,Q} \end{bmatrix}. \tag{5}$$

The structure has two extreme cases. When the signal $x(t)$ is divided into only $Q = 1$ segment, at least $P = M$ parallel paths are needed, which results higher system complexity, but the sampling rate is very low with $T_c = T$. However when the structure has only $P = 1$ path, the sampling rate becomes higher with $T_c = \frac{T}{M}$. Hence the number of parallel paths is approximately inversely proportional to the number of samples per path, which presents a tradeoff between the system complexity and the sampling rate.

### C. Recovery form subsamples

Convert the subsamples matrix $\mathbf{Y}$ to a column vector $\widetilde{\mathbf{Y}}$ as $\widetilde{\mathbf{Y}} = [\mathbf{y}_1, \mathbf{y}_2, \cdots, \mathbf{y}_P]^T$ ,where $(\cdot)^T$ indicates the transpose. And for brevity, we define the $M \times N$ matrix $\mathbf{V} = \mathbf{\Phi\Psi}$. According to (4), the element of $\mathbf{V}$ in the $m$th row and the $n$th column, where $m = (p-1)Q + q$, can be expressed as

$$\nu_{(p-1)Q+q,n} = \int_{(q-1)T_c}^{qT_c} c_p(t)\psi_n(t)dt. \tag{6}$$

Then the analog signal $x(t)$ can be recovered by solving the following problem

$$\widetilde{\mathbf{\Theta}} = arg\,min||\mathbf{\Theta}||_1 \; s.t. \; \widetilde{\mathbf{Y}} = \mathbf{V\Theta}. \tag{7}$$

In this paper, OMP is applied to reconstruct the analog signals. A short algorithmic description of OMP is listed in Table II.

## IV. Simulations

In this section, we present simulations to show the effectiveness of CM-PSCS structure and also compare the performances between the CM-PSCS and BM-PSCS structures under two different situations. We exploit normalized mean square error (NMSE) and detection percentage (DP) to reflect the system performance, where $NMSE$ is defined as

$$NMSE = \frac{\|x(t) - \widetilde{x}(t)\|^2}{\|x(t)\|^2}, \tag{8}$$

and $DP$ is expressed as

$$DP = \left(1 - \frac{\left\|\widetilde{\mathbf{\Theta}} - \mathbf{\Theta}\right\|}{\|\mathbf{\Theta}\|}\right) \cdot 100\%. \tag{9}$$

TABLE II: The short description of OMP algorithm

| | |
|---|---|
| Initialization | set non-zero elements $\mathbf{I}$ as empty, set residual error as $\mathbf{r} = \mathbf{x}$. |
| Iteration | while halting criterion false, do |
| | (1) Correlate all columns of $\mathbf{\Psi}$ with $\mathbf{r}$, choose the largest element by magnitude and add its index to $\mathbf{I}$: $i = \arg\max_i \lvert\mathbf{\Psi}_i' * \mathbf{r}\rvert, \mathbf{I} = \mathbf{I} \bigcup \{i\}$. |
| | (2) Find an estimate $\widehat{\mathbf{\Theta}}$ that minimizes $\lVert\mathbf{x} - \widehat{\mathbf{\Psi}}\widehat{\mathbf{\Theta}}\rVert$: $\widehat{\mathbf{\Theta}} = \arg\min_{\widehat{\mathbf{\Theta}}} \lVert\mathbf{x} - \widehat{\mathbf{\Psi}}\widehat{\mathbf{\Theta}}\rVert$, where $\widehat{\mathbf{\Psi}}$ is obtained from the columns in $\mathbf{\Psi}$ having indices in the set $\mathbf{I}$. |
| | (3) Update the residual:$\mathbf{r} = \mathbf{x} - \widehat{\mathbf{\Psi}}\widehat{\mathbf{\Theta}}$. |
| | end while |
| Output | The coefficient vector $\mathbf{\Theta} = \widehat{\mathbf{\Theta}}$. |

### A. Reconstruction for Time-Frequency Signals

The time-frequency signals are modulated using different frequencies at different times, as in the case of frequency hopping radios. The short-time Fourier transforms (STFT) that performs Fourier analysis of windowed versions of the input signals to establish frequency content at local time neighborhoods is used to analyse this class of signals. The STFT is written as

$$\alpha(t, f) = \langle x, \psi_{\tau,f} \rangle = \int_{-\infty}^{\infty} x(t) g(t-\tau) e^{-j2\pi ft} dt \qquad (10)$$

where $g$ is a window function with $\lVert g \rVert_2 = 1$. This formulation allows us to track changes in frequency over time. We will use a dictionary of Gabor atoms during the reconstruction of the signal to obtain a representation directly in the time-frequency domain. Thus, by using such a dictionary during CS reconstruction we obtain a spectrogram as the resulting representation.

Fig. 2 show recoveries of the time-frequency signal using the BM-PSCS structure and CM-PSCS structure, where these structures have $P = 16$ paths and sample the time-frequency signal at 12.5 of Nyquist rate. Fig. 2a shows the spectrogram of the time-frequency signal composed of two frequencies which are selected randomly. It can be shown from Fig. 2b and Fig. 2c that when the signal to noise ratio (SNR) is low, the BM-PSCS structure has better performance. However when SNR become higher, they have similar performances.

### B. Reconstruction for Multiband Signals

The multiband signal consists of $N = 4$ pairs of bands, each of width $B = 50$MHz, constructed using the formula

$$x(t) = \sum_{i=1}^{N} \sqrt{E_i B} sinc(Bt) cos(2\pi f_i t) \qquad (11)$$

where $sinc(x) = sin(\pi x)/(\pi x)$. The energy coefficients are fixed as $E_i = \{1, 2, 3, 4\}$ and the carriers $f_i$ are chosen uniformly at random in $[0, f_{Nyq}/2]$ with $f_{Nyq} = 20$GHz.

Fig. 3 shows recoveries of the multiband signal using the BM-PSCS structure and CM-PSCS structure with different paths, where the length of the chipping sequence is $L = 64$

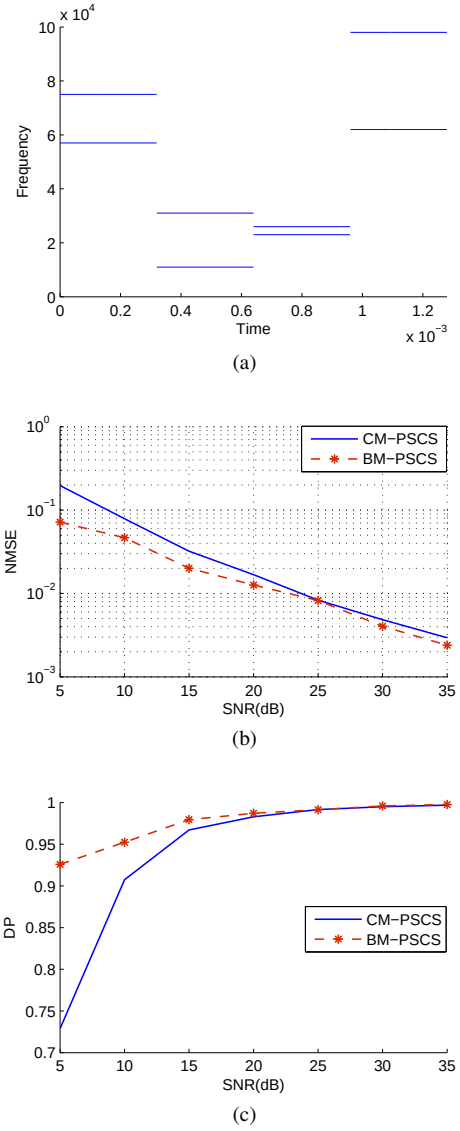


Fig. 2: Recoveries of the time-frequency signal using the BM-PSCS structure and CM-PSCS structure: (a) Spectrogram of the time-frequency signal; (b) NMSEs versus SNR for CM-PSCS and BM-PSCS; (b) DPs versus SNR for CM-PSCS and BM-PSCS.

and the sampling rate is 12.5% of the Nyquist rate. The performances of these two structures are both better when SNR becomes higher. Both structures have lower $NMSE$ and higher $DP$ when the number of paths is increased. The CM-PSCS structure has similar performance with the BM-PSCS structure under same condition.

From these two simulation examples, we can know that the BM-PSCS structure and CM-PSCS structure have better performances with more paths and higher sampling rate. The CM-PSCS structure slightly inferior to the BM-PSCS structure, but it can save more resources than the BM-PSCS structure because only 1 chipping sequence needs to be generated and

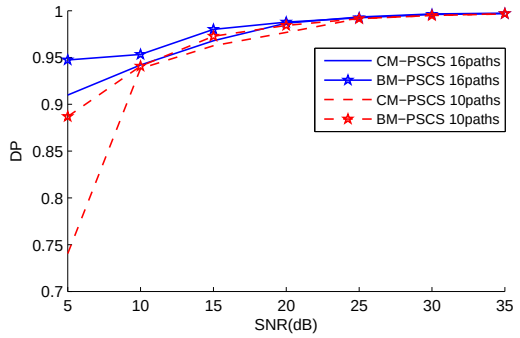


(a)

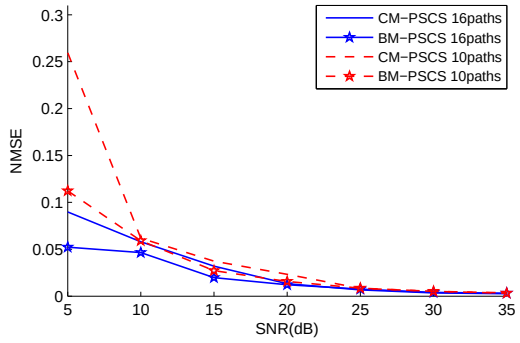


(b)

Fig. 3: Recoveries of the multiband signal using the BM-PSCS structure and CM-PSCS structure with different paths: (a) NMSEs versus SNR; (b) DPs versus SNR.

the others can be obtained by simple cyclic shift. If there are $P = 16$ paths, the BM-PSCS structure needs $16$ MLSFRs to generate chipping sequences and $16 * 64$ storage units to store them. But the CM-PSCS structure needs only $1$ MLSFR and $64$ storage units, which consumes about $1/16$ resources of those needed by the BM-PSCS structure. That is there is a trade off between the resources consumption and performance.

## V. Conclusion

Wider bandwidth is adopted in wireless communication to get high-speed data transmission. This paper improve the design of PSCS structure to sample the analog signals at a sub-Nyquist rate.

Traditionally the random Bernoulli matrix is used as the measurement matrix. However this random properties make it difficult to be implemented on hardware. Then the deterministic circulant matrix instead of the random Bernoulli matrix is adopted as the measurement matrix in this paper to reduce the resources and make AIC be easily implemented in engineering applications. We also give out the conditions should be satisfied when using circulant matrix as the measurement matrix. Compared to the BM-PSCS structure, the CM-PSCS structure has similar performance and can save more resources.

## Acknowledgment

The research is supported by China Key Projects in the National Science and Technology (NO. 2012BAF14B01, No. 2012ZX03006003-003) and National Science and Technology Major Project of the Ministry of Science and Technology (No. 2013ZX03001008).

## References

[1] E. J. Candes and M. B.Wakin, “An introduction to compressive sampling,” IEEE Signal Process. Mag., vol. 25, no. 2, pp. 21-30, Mar. 2008.

[2] D. Donoho, “Compressed sensing,” IEEE Trans. Inf. Theory, vol. 52, no. 4, pp. 1289-1306, Apr. 2006.

[3] S. Kirolos, T. Ragheb, and J. Laska, “Practical Issues in Implementing Analog-to-Information Converters,” The 6th International Workshop on System-on-Chip for Real-Time Applications, pp. 141-146, 2006.

[4] M. Mishali and Y. Eldar, “Efficient sampling of sparse wideband analog signals,” IEEE 25th Convention of Electrical and Electronics Engineers in Israel, 2008. pp. 290-294, 2008.

[5] S. Chen, D. Donoho, M. Saunders, “Atomic decomposition by basis pursuit,” SIAM Journal on Scientific Computing, vol. 20, no. 1, pp. 33-61, 1998.

[6] R. Nef, A. Zakhor, “Very low bit rate video coding based on matching pursuits,” IEEE Transaction on Circuits and Systems for Video Technology, vol. 7, no. 1, pp. 158-171, 1997.

[7] J. A. Tropp, A. C. Gilbert, “Signal Recovery From Random Measurements Via Orthogonal Matching Pursuit,” IEEE Transaction on Information Theory, vol. 53, no. 12, pp. 4655-4666, 2007.

[8] X. Chen, Z. Yu, S. Hoyos, B. M. Sadler, and J. Sil-vamartinez, A Sub-Nyquist Rate Sampling Receiver Ex-ploiting Compressive Sensing, IEEE Transactions on Circuits and Systems I: Regular Papers, vol. 58, no. 3, pp. 507-520, 2010.

[9] M. Mishali, S. Member, Y. C. Eldar, and S. Member, From Theory to Practice: Sub-Nyquist Sampling of Sparse Wideband Analog Signals, IEEE Journal of Se-lected Topics in Signal Processing, vol. 4, no. 2, pp. 375-391, 2010.

[10] Y. Zhao, X. Zhuang, H. Wang, and Z. Dai, Model-Based Multichannel Compressive Sampling with Ultra-Low Sampling Rate, Circuits, Systems, and Signal Prcessing , vol. 31, no. 4, pp. 1475-1486, 2012.

[11] Bajwa, Waheed U.; Haupt, Jarvis D.; Raz, Gil M.; Wright, Stephen J.; Nowak, Robert D., Toeplitz-Structured Compressed Sensing Matrices, IEEE/SP 14th Workshop on Statistical Signal Processing, pp. 294-298, 2007.